

GEOPHYSICAL PROSPECTING: DYNAMIC RESERVOIR CHARACTERIZATION AND TIME-LAPSE MULTICOMPONENT SEISMOLOGY FOR RESERVOIR MONITORING

Steven L. Roche

CGGVeritas, Multicomponent Processing & Technology Group

Thomas L. Davis

Colorado School of Mines, Department of Geophysics

Keywords: Multicomponent, seismology, reservoir characterization, time-lapse, P-waves, S-waves, Converted-waves, reservoir monitoring.

Contents

1. Multicomponent Seismology – Part I
 - 1.1. Rock Physics / Reservoir Processes
 2. Multicomponent Seismology – Part II
 3. Integration
 - 3.1. Multicomponent Seismic Data Acquisition
 - 3.2. Multicomponent Seismic Data Processing
 - 3.3. Integration with Well Control and Reservoir Production
 4. Key Results – Dynamic Reservoir Characterization
 - 4.1. Vacuum Field
 - 4.2. Weyburn Field
 - 4.3. Rulison Field
 5. Conclusions
- Bibliography
Biographical Sketches

Summary

Applying dynamic reservoir characterization techniques requires integrating the geologic framework of the reservoir, the reservoir processes of manipulating the fluids and pressures within the reservoir and the anticipated seismic response observed over time using surface seismic data. It is useful to gain an appreciation of general seismology in order to relate the seismic measurements to the reservoir under study. In the following sections, we present basic seismic theory, the relation to the reservoir through rock physics, and then increase the complexity of seismic theory to approach a realistic view of the reservoir framework and conditions. Being able to predict the elastic seismic response to a given reservoir state allows us to invert an observed seismic response to the actual reservoir conditions or reservoir processes. Repeated measurements over time provide the dynamic aspect of reservoir characterization, allowing prediction of future reservoir performance.

In “Multicomponent Seismology – Part I”, we introduce elastic wave propagation, relating the stress and strain of a propagating seismic wave, the stiffness tensor, the wave equation and elastic wave modes in isotropic media. Simple half-space models shows changes in P- and S-wave reflectivity due to changing fluid types in porous sandstone. Generally speaking, many reservoir time-lapse seismic signatures associated with compressibility changes in the bulk rock properties can be modeled using basic, isotropic assumptions. Examples include replacing a compressible fluid with an incompressible fluid such as a reservoir producing high GOR oil with strong water drive or water injection support. A second example would be heavy oil production using steam-assisted gravity drainage. In both of these cases, changes in bulk rock compressibility are the dominant variation over time, observable using P-wave time-lapse seismic data.

1. Multicomponent Seismology – Part I

Using P-wave (PP), S-wave (SS) and Converted-wave (PS) modes for exploration and development is a subset of elastic wave seismology. Our primary tool for observation is elastic wave propagation in the earth’s subsurface. Typically an elastic wave is generated, then observed and measured at the recording surface. The elastic wave behavior is modified by the variability of the subsurface elastic rock properties. Through our observations of the recorded elastic wavefield, we infer the changes in subsurface rock properties leading to formulate a model of the subsurface to be used for exploration. In time-lapse seismic studies for dynamic reservoir characterization, observations are repeated over time to examine temporal change in the subsurface rock properties due to reservoir processes.

First we examine the basics of elastic wave propagation based on the elastic wave equation. The elastic wave equation relates stress and strain using the stiffness of the media and describes the propagation characteristics of an elastic wave. For general elasticity, the stress field is described by a second order tensor. The stiffness of the media is represented by a fourth order tensor (the classic c_{ijkl} matrix or stiffness tensor). The interaction of the stress tensor and stiffness tensor produces the second order strain tensor. Relating stress and strain using Hooke’s Law provides the means to describe a propagating stress field.

Derivation of the elastic wave equation can be found in many seismology textbooks (Table 1). Tatham and McCormack’s (1991) description for isotropic media is a good foundation for understanding the derivation of the PP, SS and PS wave equations.

1.	Define stress and strain (both are second order tensors)
2.	Set stress and strain proportional to each other (Hooke’s Law, requires 21 independent elastic constants)
3.	Assume isotropy (Reduces to two independent elastic constants)
4.	Define forces (acting on a unit volume) from the stress, and set $F = ma$. This formula yields the equations of motion
5.	Take vector divergence of the Equation of Motion, to yield P-wave equation
6.	Take vector Curl of the Equation of Motion, to yield S-wave equation

Table 1. Outline of procedure for deriving wave equations for (linearly elastic, isotropic) P-wave and S-wave propagation. Tatham, R.H. and McCormack, M.D. (1991).

A more complete, and challenging derivation is found in Aki and Richards (1980). As in Tatham and McCormack, the elastic wave propagation characteristics are formulated under the assumption of linearly elasticity with the complexity of wave propagation embedded in the stiffness tensor of the medium and its lateral inhomogeneity. Wave propagation behaviors such as velocity, attenuation, polarization, isotropic or anisotropic are governed by the characteristics of the effective stiffness tensor. We observe both the kinematic (travel time) and dynamic (amplitude) characteristics in our observed seismic wavefield. For time-lapse seismology, it is the temporal change in the effective stiffness tensor due to reservoir processes that produces the time-lapse seismic response for analysis.

The simplest system is isotropic, meaning a given rock property such as compressibility or rigidity is invariant with direction of measurement. The stiffness tensor (c_{ijkl} matrix) reduces to the two Lamé' parameters lambda (λ) and mu (μ) which relate to compressibility and rigidity respectively. Under the isotropic assumption, these two quantities do not vary with the direction of observation. For an isotropic medium λ , μ and density (ρ) describe P-wave (V_p) and S-wave (V_s) velocity as:

$$V_p = \sqrt{\frac{\lambda + 2\mu}{\rho}} \quad V_s = \sqrt{\frac{\mu}{\rho}} \quad (1)$$

There are three wave modes, a compressional P-wave (PP) and two modes of orthogonally polarized shear waves, commonly described as SV (polarization in the vertical plane) and SH (polarization in the horizontal plane).

The Lamé' parameters λ and μ relate to elastic rock properties as:

$$\text{Shear modulus} = \mu \quad \text{bulk modulus} = k = \lambda + (2/3)\mu \quad (2)$$

Representing rigidity and compressibility of the rock, respectively.

Within the simple framework of linear elastic isotropic media, we can examine plane wave propagation behavior at an interface represented by rays perpendicular to the wave front. Consider an interface separating two homogeneous isotropic layers (Figure 1). The upper layer 1 is characterized by P-wave velocity (V_{p1}), S-wave velocity (V_{s1}) and density (ρ_1). Similarly the underlying layer 2 is characterized by V_{p2} , V_{s2} and ρ_2 .

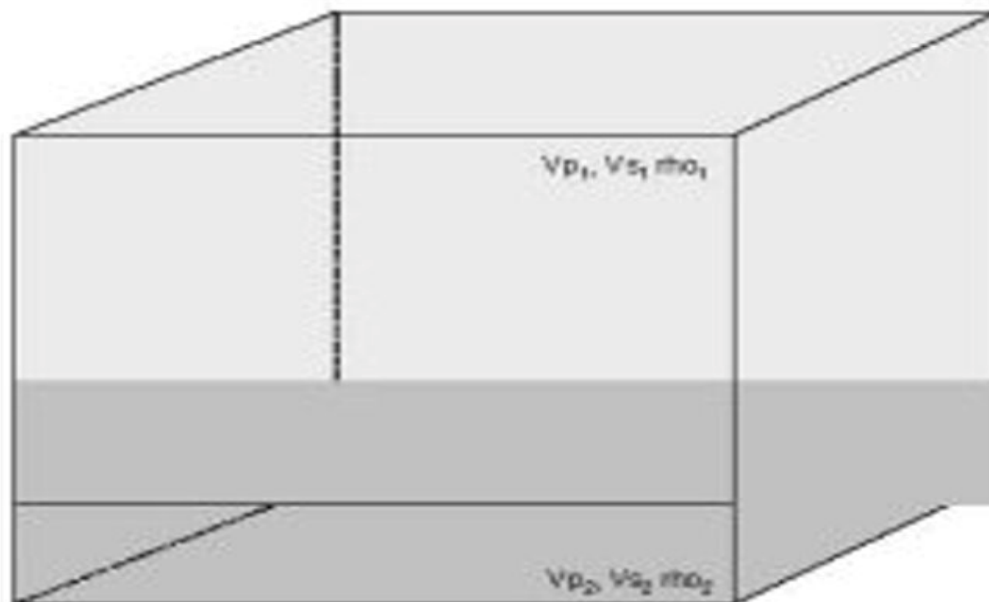


Figure 1. Simple half-space model. Two layers separated by a horizontal interface.

We can describe the three waves (PP, SV and SH) using ray diagrams. Figure 2(a) shows the generation of a P-wave at a surface location, then propagating downwards. Particle motion, delineated by the blue arrow, is along the direction of propagation. Figure 7(b) shows an S-wave (SH) with its particle motion polarized in the horizontal plane, perpendicular to the direction of propagation. Figure 2(c) shows an SV shear wave. Particle motion is in the vertical plane.

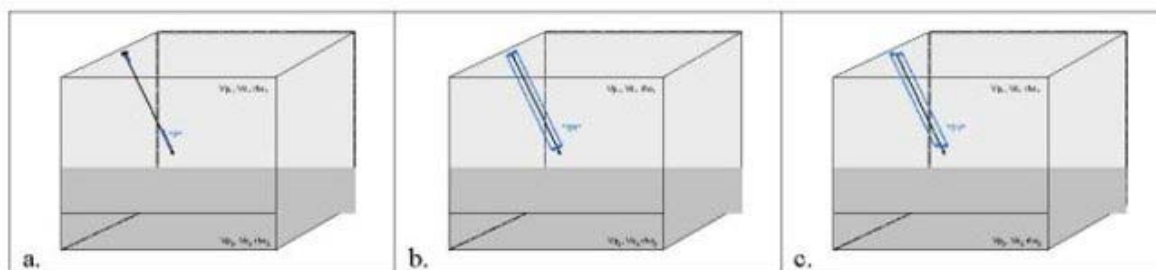


Figure 2. Three modes of downward wave propagation. P-wave (a), S-wave with horizontal polarization or SH (b) and S-wave with vertical polarization or SV (c).

A simplification is to consider just the pure mode reflection of these three waves at the interface separating layer 1 and 2 (Figure 3).

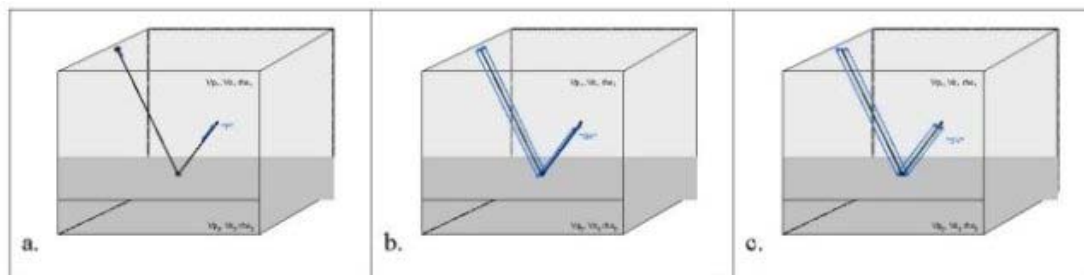


Figure 3. Pure mode reflections. P-wave (a), SH (b) and SV (c). In reality, reflection, transmission and conversion will occur for this non-normal incidence example except the SH mode will not convert to other modes under isotropic, homogeneous and horizontal interface assumptions.

Particle motion associated with the incident and reflected P-wave remains along the direction of propagation. Similarly the particle motion of the incident and reflected SV wave remains perpendicular to the direction of propagation and in the vertical plane. SH particle motion is in the horizontal plane.

In reality, even for this simple homogeneous isotropic model, an incident wave at an interface reflects, transmits and converts its energy into different wave modes depending on incident wave type, contrast in the stiffness tensor and angle of incidence. Figure 4 shows the energy partitioning in the upper half-space only (neglects transmission into lower layer 2).

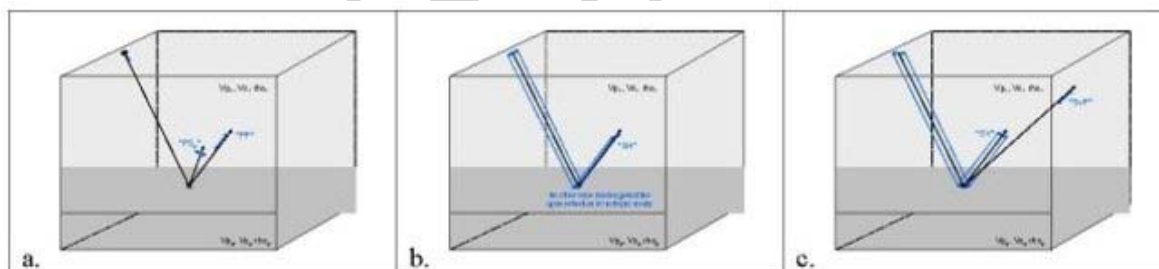


Figure 4. Possible conversion to other upgoing wave modes (transmission and conversion to downward traveling waves are not shown). P-wave reflection and SV PS conversion (a), SH only reflection (b) and SV reflection with SP conversion (c).

Angles of transmission and reflection are governed by Snell's Law and the wave mode amplitudes (or reflection/conversion coefficients) can be described using Zoeppritz equations (Aki and Richards, 2002). Note that the elastic wave characteristics (velocity, amplitude, reflection strength, etc) are what we observe and measure. The bulk rock properties are what we wish to derive from measuring the seismic data. Using half-space models we can vary the isotropic rock properties across a single horizontal interface. Using Zoeppritz equations we can compute P-wave reflectivity (R_{pp}) and Converted-wave

reflectivity (R_{ps}) versus P-wave incident angle, plus S-wave reflectivity (R_{ss}) versus S-wave incidence angle for a simple half-space model (Figure 5). In Figure 6 we alter the underlying sandstone layer to include 12% porosity, saturated with gas. Comparing the R_{pp} , R_{ss} and R_{ps} reflectivity curves in Figures 10 and 11 show the differing elastic wave response to the bulk rock property changes in k , μ and ρ . Note that both the presence of porosity and inclusion of gas in the pore space change the bulk rock properties, hence changing the stiffness tensor. Figures 5 and 6 represent non-reservoir and reservoir conditions respectively. We can simulate a reservoir process (gas production with water influx) by replacing the gas with incompressible brine, then recomputing the stiffness tensor. Figure 7 shows the change in R_{pp} , R_{ss} and R_{ps} . Since the reservoir process primarily produces a change in compressibility, the R_{pp} curve exhibits the dominate change over time.

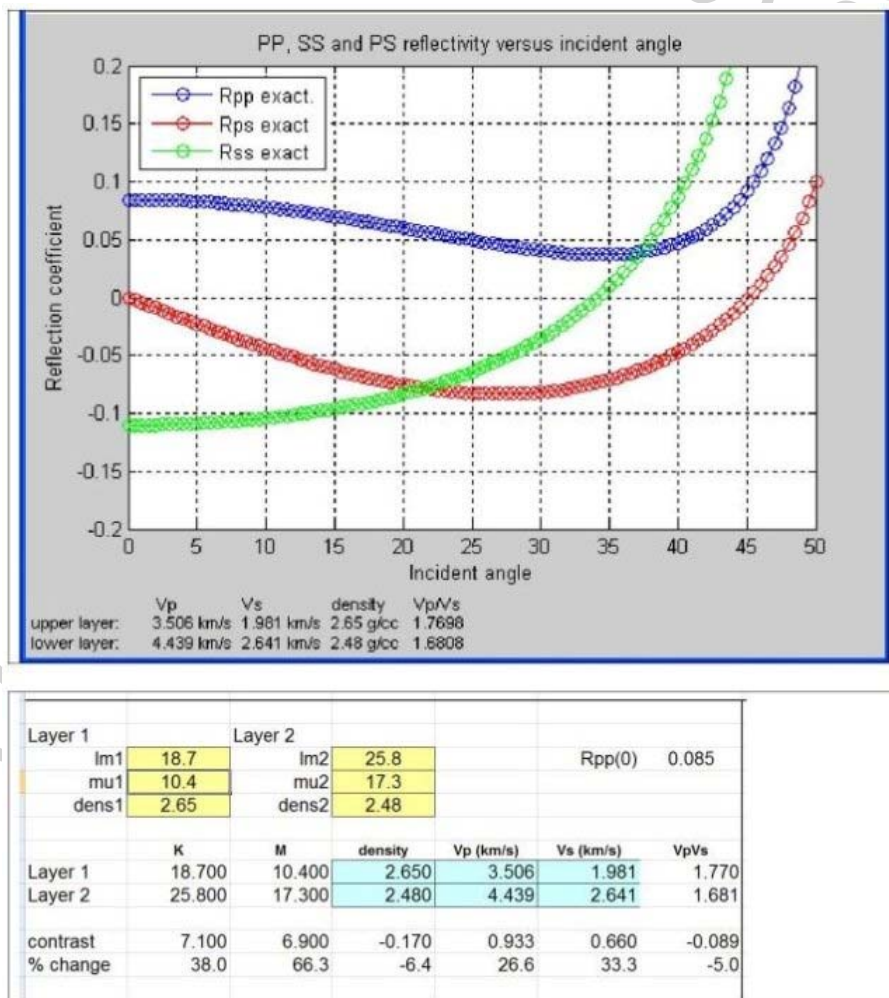


Figure 5. Half-space modeling for a shale – sand interface. Rock properties, V_p , V_s and V_p/V_s ratio are listed in the imbedded table. Reflectivity for P-wave (R_{pp}), S-wave (R_{ss}) and Converted-wave (R_{ps}) based on Zoeppritz equations are plotted vs incidence angle.

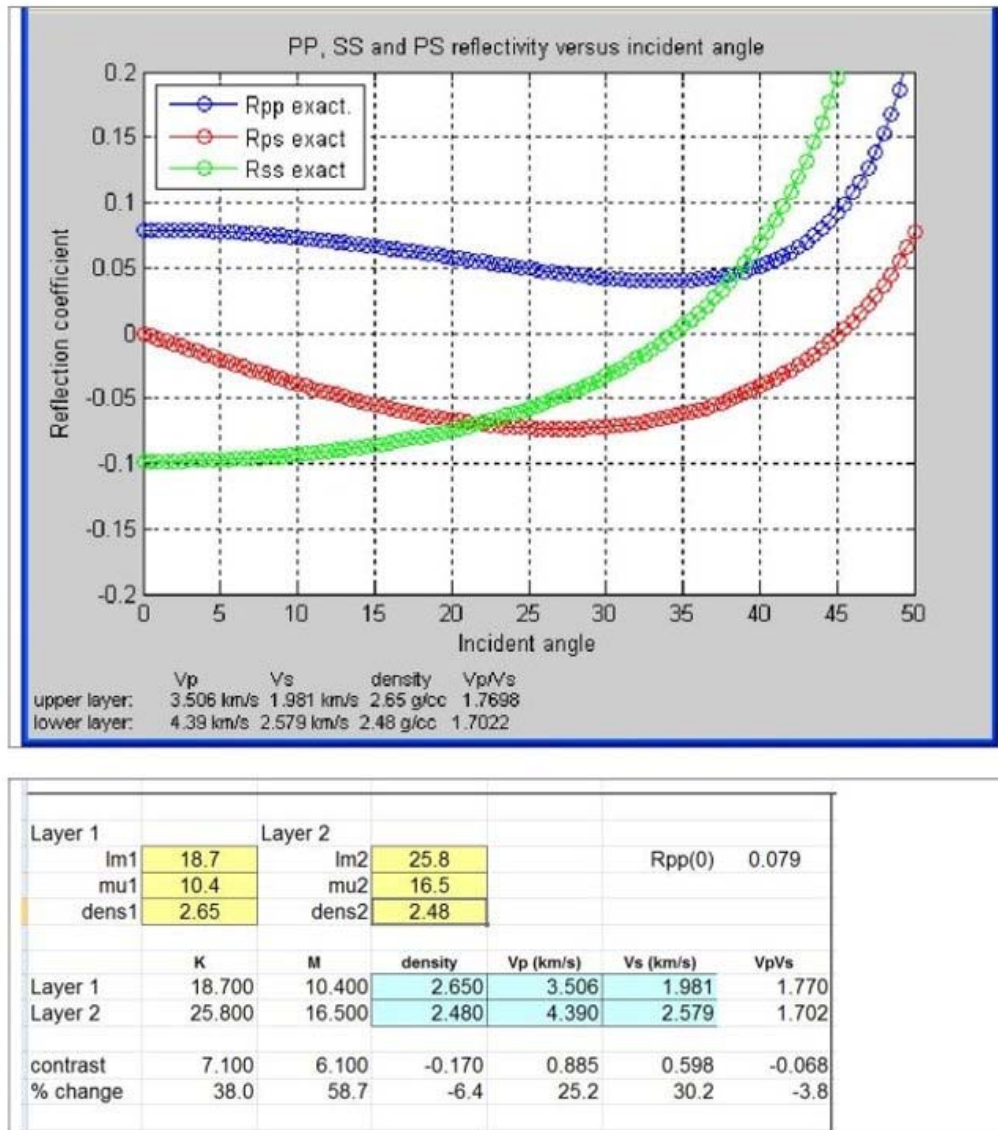


Figure 6. Half-space modeling for a 12% porosity sandstone (gas-saturated) overlain by shale. These rock property values are consistent with the model in Figure 5 being altered to include 12% porosity sandstone with gas-saturated pore space.

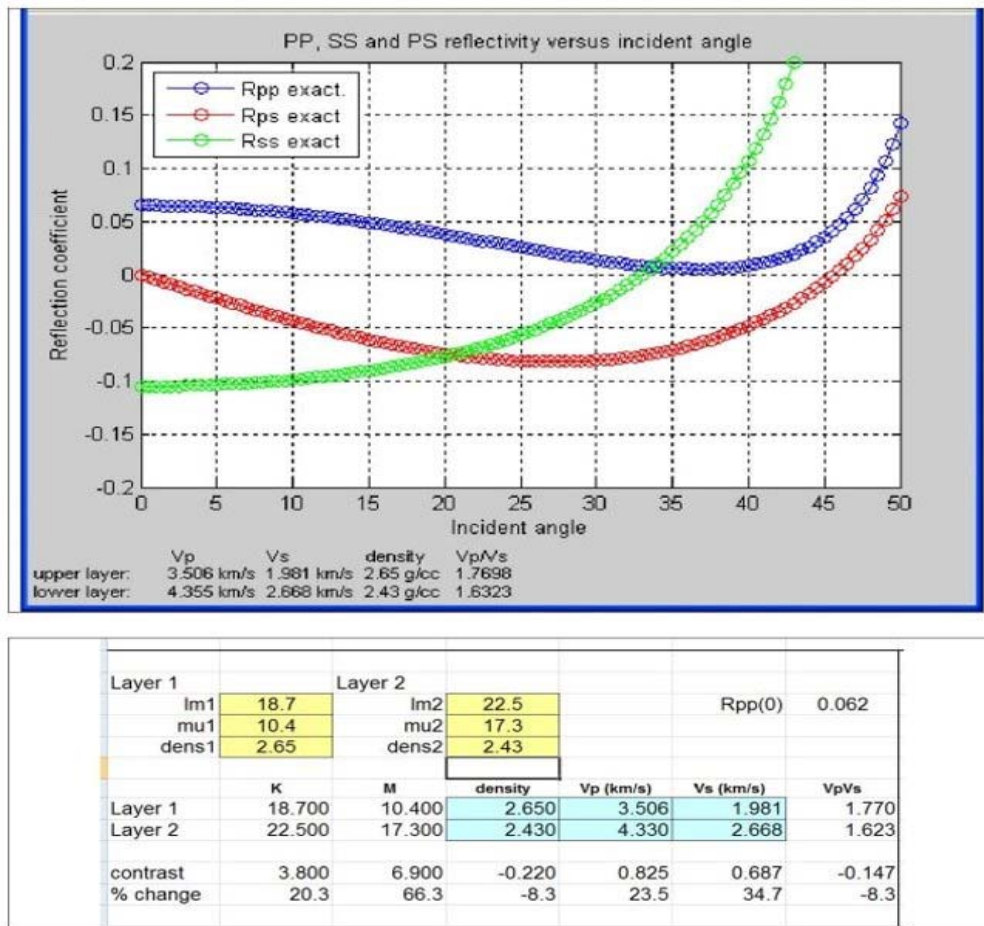


Figure 7. Half-space modeling for a 12% porosity sandstone (brine-saturated) overlain by shale. Comparing the Rpp, Rss and Rps curves with those in Figure 6 show a significant change in Rpp with minimal effect on Rss and Rps. This is consistent with a reservoir process replacing a compressible gas with an incompressible fluid.

TO ACCESS ALL THE 37 PAGES OF THIS CHAPTER,
 Visit: <http://www.eolss.net/Eolss-sampleAllChapter.aspx>

Bibliography

References

Adam L. and Batzle, M. (2008). *Elastic properties of carbonates from laboratory measurements at seismic*

and ultrasonic frequencies. The Leading Edge, 27, no. 8, 1026-1032. [A companion paper on the effect of fluid properties on shear wave propagation]

Adam, L., Batzle, M., and Brevik, I. (2006). *Gassmann's fluid substitution and shear modulus variability in carbonates at laboratory seismic and ultrasonic frequencies*. Geophysics, 71, no. 6, F173-F183. [Excellent paper demonstrating the effect of fluid properties on shear wave propagation]

Aki, K. and Richards, P.G. (1980). *Quantitative Seismology – Theory and Methods*. Freeman and Company. [A key reference on seismic theory and quantitative methods]

Batzle, M.B., Han D. and Hofmann, R. (2006). *Fluid mobility and frequency-dependent seismic velocity – Direct measurements*. Geophysics, 71, no. 1, N1-N9. [Good reference paper demonstrating the effect of fluid properties on shear wave propagation]

Batzle, M.B., Han D. and Hofmann, R. (2006). *Heavy oils—seismic properties*. The Leading Edge, 25, no. 6, 750-756. [Good discussion outlining the effect of fluid properties on shear wave propagation]

Bourbie, T., Coussy, O. and Zinszner, B. (1986). *Acoustics of Porous Media*, IFP Publication. [A key reference on the petrophysics of porous rock]

Brown, L.T., Davis, T.L. and Batzle, M.B. (2002). *Integration of rock physics, reservoir simulation, and time - lapse seismic data for reservoir characterization at Weyburn Field, Saskatchewan*. SEG, Expanded Abstracts, 21, no. 1, 1708-1711. [Good example for integrating seismic measurements and rock physics for reservoir monitoring]

LaBarre, E.A. and Davis, T.L. (2008). *Fault and natural fracture identification from multicomponent seismic at Rulison Field, Colorado*. SEG, Expanded Abstracts, 27, no. 1, 948-952. [Example of using S-wave seismic anisotropy measurements to characterize a low-porosity, fractured sandstone reservoir]

Lynn, H.B. (2004). *The winds of change*. The Leading Edge, 23, no. 11, 1156-1162. [Part 1 of a two-part series on relating seismic anisotropy measurements to relative fluid flow characteristics in porous media]

Lynn, H.B. (2004). *The winds of change: Anisotropic rocks—their preferred direction of fluid flow and their associated seismic signatures—Part 2*. The Leading Edge, 23, no. 12, 1258-1268. [Part 2 of a two-part series on relating seismic anisotropy measurements to relative fluid flow characteristics in porous media]

MacBeth, C. and Lynn, H.B. (2000). *Applied seismic anisotropy: Theory, background, and field studies*. SEG Books, 725-725. [Good compilation of papers on seismic anisotropy theory with example applications]

Shuck, E.L., Davis, T.L. and Benson, R.D. (1996). *Multicomponent 3-D characterization of a coalbed methane reservoir*. Geophysics, 61, no. 2, 315-330. [Good reference paper on measuring shear wave anisotropy using surface seismic multicomponent data]

Tatham, R.H. and McCormack, M.D. (1991). *Multicomponent Seismology in Petroleum Exploration*. SEG Books, 1-248. [Excellent handbook for multicomponent seismic methods from theory, through acquisition, processing and interpretation]

Tsvankin, I. (2001). *Seismic Signatures and Analysis of Reflection Data in Anisotropic Media. Handbook of Geophysical Exploration – Seismic Exploration*. Vol. 29. [A compilation of I. Tsvankin's course notes on seismic anisotropy, a key reference document]

Wang, Z. (2001). *Fundamentals of seismic rock physics*. Geophysics, 66, no. 2, 398-412. [Excellent overview paper relating petrophysics and seismic measurements]

Winterstein, D.F. (2000). *Velocity anisotropy terminology for geophysicists*. SEG Books, 20, 47-65. [Good reference paper for defining anisotropy terminology]

Related Papers

Vacuum Field

Roche, S. L., Davis, T. L. and Bell, C. R. (2000). *An onshore time-lapse (4-D), multicomponent, data processing case history, Vacuum Field, New Mexico, Applied seismic anisotropy: theory, background, and field studies*. 20: Soc. of Expl. Geophys., 718-721. [Case history on multicomponent processing techniques for time-lapse seismic data]

Talley, D. J., Davis, T. L., Benson, R. D. and Roche, S. L. (1998). *Dynamic reservoir characterization of Vacuum Field*. The Leading Edge, 17, no. 10, 1396-1402. [Case history on using repeated multicomponent seismic data to monitor a CO₂ injection program in a carbonate reservoir]

Weyburn Field

Davis, T. L., Terrell, M.J., Benson, R. D., Cardona, R., Kendall, R. R. and Winarsky, R. (2003). *Multicomponent seismic characterization and monitoring of the CO₂ flood at Weyburn Field, Saskatchewan*. The Leading Edge, 22, no. 7, 696-697. [Case history using time-lapse multicomponent seismic data to monitor a CO₂ injection program at Weyburn Field, Saskatchewan]

Kendall, R. R., Winarsky, R., Davis, T. L. and Benson, R. D. (2003). *9C, 4D Seismic Processing for the Weyburn CO₂ Flood, Saskatchewan, Canada*. Recorder, 28, no. 8, 40-44. [Seismic processing techniques for time-lapse multicomponent data]

Rulison Field

Davis, T.L. (2007). *Let's get cracking*. The Leading Edge, 26, no. 2, 160-161. [Case history on using time-lapse multicomponent data to monitor pressure-depletion response in a low-porosity sandstone reservoir]

Biographical Sketches

Steven L. Roche, PhD, is Geophysical Advisor for the Multicomponent Processing & Technology Group – CGGVeritas. He holds a PhD Geophysics degree from the Colorado School of Mines. His thesis topic and research interests are multicomponent seismology for time-lapse applications for reservoir characterization and monitoring. He acted as SEG Vice-President (1999-2000), served as Associate Editor (Data Acquisition) for GEOPHYSICS and currently is a member of the SEG Scholarship Committee.

Thomas L. Davis, PhD, is a Professor of Geophysics at Colorado School of Mines and Director of the Reservoir Characterization Project. He is active in the Society of Exploration Geophysicists as an organizer for technical conferences, workshops and continuing education programs and has served as SEG's Second Vice President, Technical Program Chairman, and Distinguished Lecturer. He received the C.J. Mackenzie Award from the Engineering College of the University of Saskatchewan, the Milton B. Dobrin Award from the University of Houston, and the Dean's Excellence and Melvin F. Coolbaugh Memorial Awards from the Colorado School of Mines. He was a co-recipient of the best poster award of the SEG in 2009 for a presentation on multicomponent seismic applications to tight gas fractured reservoir characterization.